Journal of Coastal and Marine Engineering
Volume 1 • Number 1 • June 2018

Numerical Simulation of Tidal Wave over Wavy Bed

Maryam Ziaadini-Dashtekhaki[1], Mahnaz Ghaeini-Hessaroeyeh[2*]

1) M.Sc. Graduate, Department of Civil Engineering, Faculty of Engineering, Shahid Bahonar University of Kerman, Kerman, Iran, m.ziaadini@eng.uk.ac.ir

2) Assistant Professor, Department of Civil Engineering, Faculty of Engineering, Shahid Bahonar University of Kerman, Kerman, Iran, mghaeini@uk.ac.ir (Corresponding author)

Abstract: The HLLC method is a good approximate Riemann solver that has the ability to resolve shock, contact and rarefaction waves. High-order accuracy is achieved by using Total Variation Diminishing version of Weighted Average Flux (TVD-WAF) explicit method. The bed topography and friction source terms are treated in a fully implicit method. The accuracy of the scheme has been verified by the implementation of several computational tests. The results show appropriate agreement of the present model results with the exact and analytical solutions.

Keywords: Numerical model, shallow water equations, TVD-WAF, tidal wave, roll-waves.

1. Introduction

A common method for modeling water flows with free surface is to solve the shallow water equations, which can be obtained from depth averaging of the Navier Stokes equations where the hydrostatic pressure distribution is assumed. The equations consist of a system of nonlinear conservation laws of mass and momentum. There are many numerical approaches for solving the mentioned equations. One of the popular shock-capturing methods is the Godunov-type scheme. Godunov scheme is based on the Riemann solution using the exact or approximate Riemann solver. This scheme assumed that conservative variables are piecewise constant over the mesh cells at each time step, and the time averaged flux function is determined by the exact solution of the local Riemann problem at the cell interface [1]. The original Godunov scheme is first-order accurate and an iterative method is required because the Riemann problem has no closed form solution [1]. Approximate state Riemann solvers do not require iterative processes, thus, these solvers are more useful. This scheme is widely used for example for Roe, HLL, HLLE and HLLC schemes [1, 2, 3]. This paper is focused on the treatment of the source term on roll-wave and tidal wave over the wavy bed in the present model. Numerous researches have been done on tidal flow modeling. Zhou et al (2001) proposed the surface gradient method (SGM) for solving the source term in the shallow water equations and modeling the tidal flow [4]. Pu et al. (2012) employed the HLLC method that has a first-order accuracy and modeled the tidal wave. They used Surface Gradient Upwind Method (SGUM) for modeling the bed topography [5]. Devkota and Fang (2015) implemented a 3D numerical simulation of flow dynamics in a tidal river [6]. Huang et al. (2015) performed 3D simulation to investigate flow and transport mechanisms through submerged vegetation under the influence of tidal oscillations [7]. Analytical solution and numerical simulation of evolution of roll-waves are reported by Dressler (1949) and Que & Xu (2006) respectively [8, 9]. Que and Xu (2006) introduced a finite volume kinetic BGK scheme to study of roll-waves. This scheme is based on the numerical solution of the gas-kinetic Bhatnagar-Gross-Krook model in the flux evaluation across each cell interface [8]. In the present study, the 1D shallow water equations are used and the trapezoidal time integration method is used to implement the source term. The HLLC method is selected for flux modeling. The TVD-WAF method is selected to achieve the second-order accuracy. Several computational tests have been chosen to demonstrate the capability of the present model.

2. Numerical Model

2.1. Governing Equations

The one-dimensional shallow water equations with bottom topography expressed in the conservation law form are given by Equation (1) and the free surface elevation is given by Equation (2).

$$\frac{\partial h}{\partial t}+\frac{\partial}{\partial x}(hu)=0$$

$$\frac{\partial}{\partial t}(hu)+\frac{\partial}{\partial x}(hu^2+\frac{1}{2}gh^2)=-gh\frac{dB}{dx} \quad (1)$$

$$\eta(x,t)=h(x,t)+B(x) \quad (2)$$

Where t denotes the time, x is the distance, h (x,t) is the water depth above the bottom, u(x,t) is the water velocity average across the water depth in the x-direction, and g is the acceleration due to gravity, given by the constant value g=9.81m/s^2. B=B(x) is the bottom elevation.

*Corresponding author.

2.2 Discretization

Equation (1) in the form of hyperbolic conservation equations can be written as:

$$\frac{\partial U}{\partial t}+\frac{\partial F}{\partial x}=S \tag{3}$$

The discretization of Eq. (3) is as follows:

$$U_i^{n+1}=U_i^n-\frac{\Delta t\,(F_{i+1/2}-F_{i-1/2})^n}{\Delta x} \tag{4}$$

Where Δt is the time step, Δx is the spatial step, n+1 is the new time level; n represents the state updated from Eq. (3), and $F_{i+1/2}$ and $F_{i-1/2}$ are the interface fluxes. The Harten-Lax-van Leer-Contact (HLLC) approximate Riemann solver [10] is adopted in the present model. $F_{i+1/2}$ is evaluated as follows:

$$F_{i+1/2}=\begin{cases}F_L & if \quad s_L\ge 0\\ F_{*L} & if \quad s_L\le 0\le s_*\\ F_{*R} & if \quad s_*\le 0\le s_R\\ F_R & if \quad s_R\le 0\end{cases} \tag{5}$$

Where $F_L=F(U_L)$, $F_R=F(U_R)$, U_L, U_R are the left and right Riemann states of a local cell interface, respectively, F_{*L} and F_{*R} are the numerical fluxes in the left and right sides of the star region. S_L, S_* and S_R are the speed of the left, contact and right waves, respectively. There are several possible options for these wave speeds. The approach proposed by Toro (2001) is:

$$\begin{aligned}S_R&=\max(u_R+\sqrt{gh_R},u^*+\sqrt{gh^*})\\ S_L&=\min(u_L-\sqrt{gh_L},u^*-\sqrt{gh^*})\end{aligned} \tag{6}$$

In the above expressions h^* and u^* are the flow depth and flow velocity in the intermediate region of the wave structure. One can evaluate these flow variables as follows [11]:

$$\begin{aligned}h^*&=\frac{1}{g}\left[\frac{1}{2}(\sqrt{gh_L}+\sqrt{gh_R})+\frac{1}{4}(u_L-u_R)\right]^2\\ u^*&=\frac{1}{2}(u_L+u_R)+\sqrt{gh_L}-\sqrt{gh_R}\end{aligned} \tag{7}$$

In order to achieve second-order accuracy the Weighted Average Flux (WAF) method which was introduced by Toro (2001) is employed in the present model.

The WAF scheme, because of second-order accuracy in space and time, produces spurious oscillations near steep gradients, and so it needs TVD stabilization [11]:

$$\begin{aligned}F_{i+1/2}^{TVDWAF}&=\frac{1}{2}(F_i+F_{i+1})-\frac{1}{2}\sum_{k=1}^{3}sign(c_k)A_{i+\frac{1}{2}}^{(k)}\Delta F_{i+\frac{1}{2}}^{(k)}\\ F_i&=F(U),\ \Delta F_{i+\frac{1}{2}}^{(k)}=F_{i+\frac{1}{2}}^{(k+1)}-F_{i+\frac{1}{2}}^{(k)},\ c_k=(\frac{\Delta t}{\Delta x})s_k\end{aligned} \tag{8}$$

Where $A^{(k)}_{i+1/2}$ is a WAF flux limiter function. Some suitable choices for limiter function are reported. The Van Leer limiter [11] has been used in the present model:

$$A_{vl}(r,|c|)=\begin{cases}1 & \text{if} \quad r\le 0\\ 1-\dfrac{(1-|c|)2r}{1+r} & \text{if} \quad r\ge 0\end{cases} \tag{9}$$

$$r^{(k)}=\begin{cases}\dfrac{\Delta h_{i-1/2}^{(k)}}{\Delta h_{i+1/2}^{(k)}}=\dfrac{h_i^{(k)}-h_{i-1}^{(k)}}{h_{i+1}^{(k)}-h_i^{(k)}} & if \quad c_k>0\\ \dfrac{\Delta h_{i+3/2}^{(k)}}{\Delta h_{i+1/2}^{(k)}}=\dfrac{h_{i+2}^{(k)}-h_{i+1}^{(k)}}{h_{i+1}^{(k)}-h_i^{(k)}} & if \quad c_k<0\end{cases} \tag{10}$$

2.3 Treatment of the Source Term

The splitting schemes are concerned for solving nonlinear system of hyperbolic conservation laws with source term. A second-order accurate splitting scheme is selected and three initial value sub-problems are used and are calculated by the following relations:

$$\begin{cases}ODEs: \ \dfrac{dU}{dt}=S(U) & \underrightarrow{\Delta t'}\ U^{(1)}\\ ICs: \ U^n\end{cases} \tag{11}$$

$$\begin{cases}PDEs: \ \dfrac{\partial U}{\partial t}+\dfrac{\partial F}{\partial x}=0 & \underrightarrow{\Delta t}\ U^{(2)}\\ ICs: \ U^1\end{cases} \tag{12}$$

$$\begin{cases}ODEs: \ \dfrac{dU}{dt}=S(U) & \underrightarrow{\Delta t'}\ U^{n+1}\\ ICs: \ U^{(2)}\end{cases} \tag{13}$$

Where n is the current time level and $\Delta t'=\Delta t/2$. Indeed, for inhomogeneous system (3), first the initial value problem (11) which is the Ordinary Differential Equation (ODE) is solved. In the second step, the Partial Differential Equation (PDE) is solved and its initial condition is the actual initial condition equation (11). Finally the ODE (13) is solved and U is calculated at the new time level. The above splitting procedure can be expressed in the succinct form:

$$U^{n+1}=S^{(\Delta t')}H^{(\Delta t)}S^{(\Delta t')}U^n \tag{14}$$

In which S and H indicate the splitting operators for the source term and homogeneous term, respectively [12]. In the present work the trapezoidal time integration method is used to solve the source term. This operator is second-order accurate as follows [13]:

$$U_i^{(1)}=U_i^n+\frac{\Delta t}{2}\left[S(U_i^{(1)})+S(U_i^n)\right] \tag{15}$$

$$S(U_i^{(1)})=S(U_i^n)+(\frac{\partial S(U)}{\partial U})_i^n\Delta U_i+o(\Delta t')^2 \tag{16}$$

$$\Delta U_i = U_i^{(1)} - U_i^n \tag{17}$$

The second term of the right-hand side of the Equation (16) is the Jacobian matrix of the source term:

$$\left(\frac{\partial S(U)}{\partial U}\right)_i^n = \begin{bmatrix} 0 & 0 \\ g\left(s_0 + \frac{7}{3}\frac{n^2 u|u|}{h^{4/3}}\right)_i^n & -2g\left(\frac{n^2|u|}{h^{4/3}}\right)_i^n \end{bmatrix} \tag{18}$$

After some algebraic handwork, the Equation (19) can be derived [13]:

$$\left[I - \frac{\Delta t'}{2}\left(\frac{\partial S(U)}{\partial U}\right)_i^n\right]\Delta U_i = \Delta t' S(U_i^n) \tag{19}$$

Where I is the identity matrix. Equation (19) is expanded to give:

$$\begin{bmatrix} p_{11} & p_{12} \\ p_{21} & p_{22} \end{bmatrix}\begin{bmatrix} h_i^{(1)} - h_i^n \\ (hu)_i^{(1)} - (hu)_i^n \end{bmatrix} = \begin{bmatrix} R_1 \\ R_2 \end{bmatrix} \tag{20}$$

Where

$$\begin{bmatrix} p_{11} & p_{12} \\ p_{21} & p_{22} \end{bmatrix} = \begin{bmatrix} 1 & 0 \\ -\frac{\Delta t}{4} g\left(s_0 + \frac{7}{3}\frac{n^2 u|u|}{h^{4/3}}\right)_i^n & 1 + \frac{\Delta t}{2} g\left(\frac{n^2|u|}{h^{4/3}}\right)_i^n \end{bmatrix} \tag{21}$$

And

$$\begin{bmatrix} R_1 \\ R_2 \end{bmatrix} = \begin{bmatrix} 0 \\ \frac{\Delta t}{2} g h_i^n (s_0 - (s_f)_i^n) \end{bmatrix} \tag{22}$$

The solution of Equation (20) is:

$$\begin{cases} h_i^{(1)} = h_i^n \\ (hu)_i^{(1)} = (hu)_i^n + \dfrac{R_2}{p_{22}} \end{cases} \tag{23}$$

2.4 Numerical Stability

The TVD-WAF is the explicit scheme therefore the Courant-Friedrichs-Lewy (CFL) criterion must be calculated. For stability, The CFL number is a necessary condition for solving the hyperbolic PDEs. To define the appropriate time step at each discrete time level, the following formula has been used:

$$\Delta t = C_r \min\left(\frac{\Delta x}{|u_i| + \sqrt{g h_i}}\right) \tag{24}$$

Where C_r is the CFL number. For stability, the following condition must be set:

$$0 < C_r \le 1 \tag{25}$$

3. Cmputational Tests

3.1 Dam-Break

In the test 1 the length of the channel is 50 m and the initial conditions are given in Table 1. The computations are performed with $\Delta x = 0.5$ m and C_r=0.6. The initial conditions for this test are in such a way that the solution consists of two strong rarefaction waves travelling in opposite directions and a portion of dry bed between them. Many studies have shown that various methods will compute a negative depth h in the vicinity of very shallow water or dry bed produced by strong rarefactions [11]. Comparison of the model results and the exact solution of Toro indicates the good performance of the model in the treatment of the two rarefactions and generation of a dry bed (Figure 1).

Table 1. The initial data for dam-break test

Test	h_L (m)	u_L (m/s^2)	h_R (m)	u_R (m/s^2)	X_0 (m)	t_{out} (s)
1	1.0	-3.0	1.0	3.0	25.0	5.0
2	0.0	0.0	1.0	0.0	30.0	4.0

Where X_0 is the location of the dam, H_L and H_R are the water depth on the left and right of the dam, respectively. U_L and U_R are the velocity on the left and right of the dam, respectively [11].

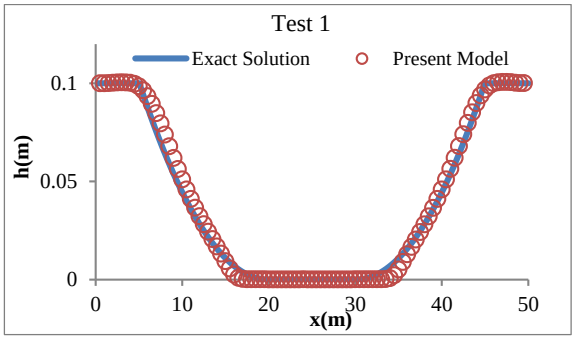

Figure 1. Comparison of the result of the present model and exact solution of Toro for the profile of depth

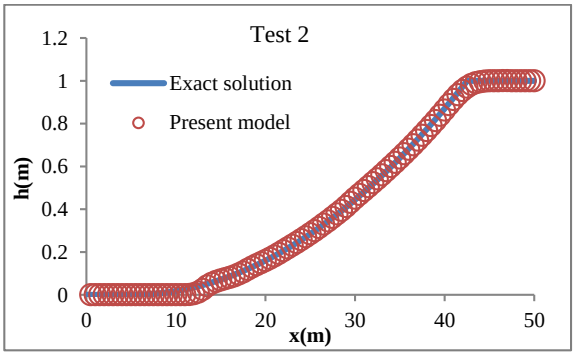

Figure 2. Comparison of the present model results and the exact solution of Toro for the profile of depth

Test 2 is the dam-break problem with left dry bed. The solution consists of a single right rarefaction wave with the wet/dry front that is attached to its tail. The length of the channel is 50 m and the initial conditions are presented in Table 1. The propagation of wet/dry front at the correct speed is one major difficulty of numerical methods. In a real application in which such fronts are to be propagated by several kilometers, the propagation speed and thus the predicted wave arrival time will be a considerable challenge for numerical methods [11]. The results of the model are shown in Figure 2. The model results have a good agreement with the exact solution of Toro [11], especially in the beginning of the rarefaction part, but most of the models with the second-order accuracy are more diffusive in this part.

3.2 Tidal Wave Flow

Generally, Tidal waves have to be considered in coastal engineering. In the present study, the problem that its analytical solution is reported by Bermudez and Vazquez [14] is selected. The bed topography is defined by the sine function:

$$H(x) = 50.5 - \frac{40x}{L} - 10\sin\left[\pi\left(\frac{4x}{L} - \frac{1}{2}\right)\right] \tag{26}$$

Where L=14000 m is the channel length and the initial and boundary conditions are:

$$\begin{aligned} &h(x,0) = H(x) \\ &u(x,0) = 0 \end{aligned} \tag{27}$$

And

$$h(0,t) = H(0) + 4 - 4\sin\left[\pi\left(\frac{4t}{86400} + \frac{1}{2}\right)\right] \tag{28}$$

$$u(L,t) = 0$$

Also, the same bed and flow condition were used by Bermudez and Vazquez [14]. Bermudez suggested that the asymptotic analytical solution for this test as follows:

$$\begin{aligned} h(x,t) &= H(x) + 4 - 4\sin\left[\pi\left(\frac{4t}{86400} + \frac{1}{2}\right)\right] \\ u(x,t) &= \frac{(x-L)\pi}{5400h(x,t)}\cos\left[\pi\left(\frac{4t}{86400} + \frac{1}{2}\right)\right] \end{aligned} \tag{29}$$

A comparison of the numerical results with the asymptotic analytical solution at t=7552.13S is shown in Figure 3 and 4.

Figures 3 and 4 show good agreement between the analytical results and the results of the present model for both the water surface and velocity profile.

Furthermore, the results of the present model are compared with the results of Pu et al. (2012), for this test. In the present model, the TVD-WAF method that has second-order accuracy both in space and time is used and the trapezoidal time integration method is employed to implement the source term. Pu et al. (2012) used the HLLC method that has a first-order accuracy and the Surface Gradient Upwind Method (SGUM) for modeling the bed topography.

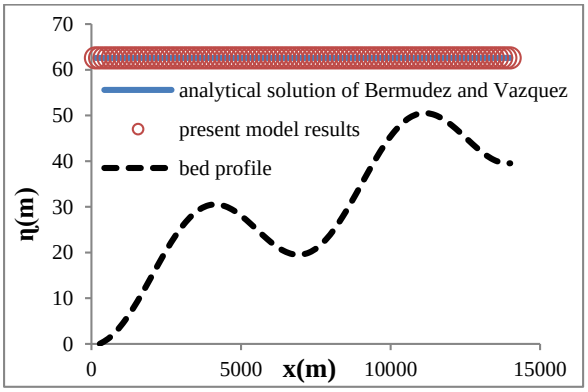

Figure 3. Comparison of the result of the present model and analytical solution of Bermudez and Vazquez for water surface.

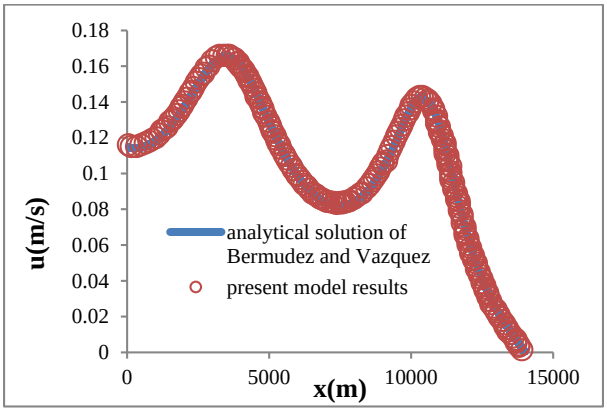

Figure 4. Comparison of the result of the present model and analytical solution of Bermudez and Vazquez for velocity.

The average relative error and Root Mean Square Error (RMSE) for the present model results and the results of Pu et al.(2012) are presented in Table 2. As can be observed in this table, the present model results are more accurate than the model results of Pu et al.(2012).

Table 2. The Calculated Average relative errors and RMSEs for the simulated water surface compared to the experimental data

	Average relative error(%)	RMSE (m)
Present model	0.95	0.0014
Pu et al. (2012) model	1.3	0.0022

3.3 Roll Waves in Inclined Open Channels

When a small perturbation imposed on the steady and uniform state flow, the flow finally evolves into a series

of breaking waves or bores that are called "roll-waves". In this test, the problem of roll-waves down an inclined open channel model is studied by Dressler firstly [8]. When roll-waves propagate downward, the water flow continuously transits from subcritical to supercritical flow and transmits back to subcritical flow again and again through a hydraulic jump (or shock). In this test, rolling waves are formed by applying a sine perturbation on the flow. The initial conditions of the water height and velocity are given by Equations (30) and (31) respectively [9]:

$$h(x,0) = h_0\left[1+\varepsilon\sin(k_w x)\right] \tag{30}$$

$$u(x,0) = u_0 + r_p\varepsilon\sin(k_w x + \theta_p) \tag{31}$$

Where ε is an amplification factor of the initial disturbance of the water height, k_w is the wave number, h_0 is the initial water height and u_0 is the initial velocity. Other parameters are as follows [9]:

$$r_p = \left|\frac{\omega}{k_w} - u_0\right|$$

$$\theta_p = \arg\left(\frac{\omega}{k_w} - u_0\right)$$

$$\omega = \frac{-\beta + \sqrt{\beta^2 - 4\gamma}}{2}$$

$$\beta = -2u_0 k_w + \frac{2C_f u_0}{h_0} i$$

$$\gamma = (u_0^2 + gh_0)k_w^2 - \frac{3C_f u_0^2}{h_0} k_w i \tag{32}$$

Where the θ_p is the phase lag between the initial water height and velocity perturbation [9].

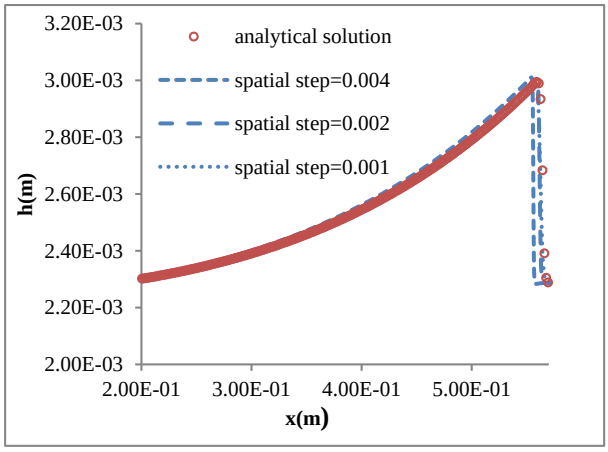

Figure 5. Sensitivity analyses of the present model applied in the numerical test of progressing roll wave.

Three numerical tests are conducted using the same parameter values with different cell sizes of 0.001, 0.002 and 0.004 m. Figure 5 illustrates the water depth in a single rolling wave that converged with the analytical solution. As can be observed in Figure 5, the solution with coarse cell sizes shows that the wave deviates from the original position. By decreasing the cell size to 0.002m, the error decreases. When the cell size is decreased to 0.001m, no considerable improvement is observed in the results as shown in Figure 5. Therefore, to reduce the computational time, the mesh size of 0.002m is selected.

Figure 6 demonstrates the evolution of roll-waves down an inclined open channel for ε=0.005, k_w=10π, C_f=0.006, Q_0=0.001m^3s^{-1}, g=9.81 m/s^2 and F_0=2.5 with the present model at t=0s and the subsequent growth in time at t=4, 8, 10, 12, 16 and 20S.

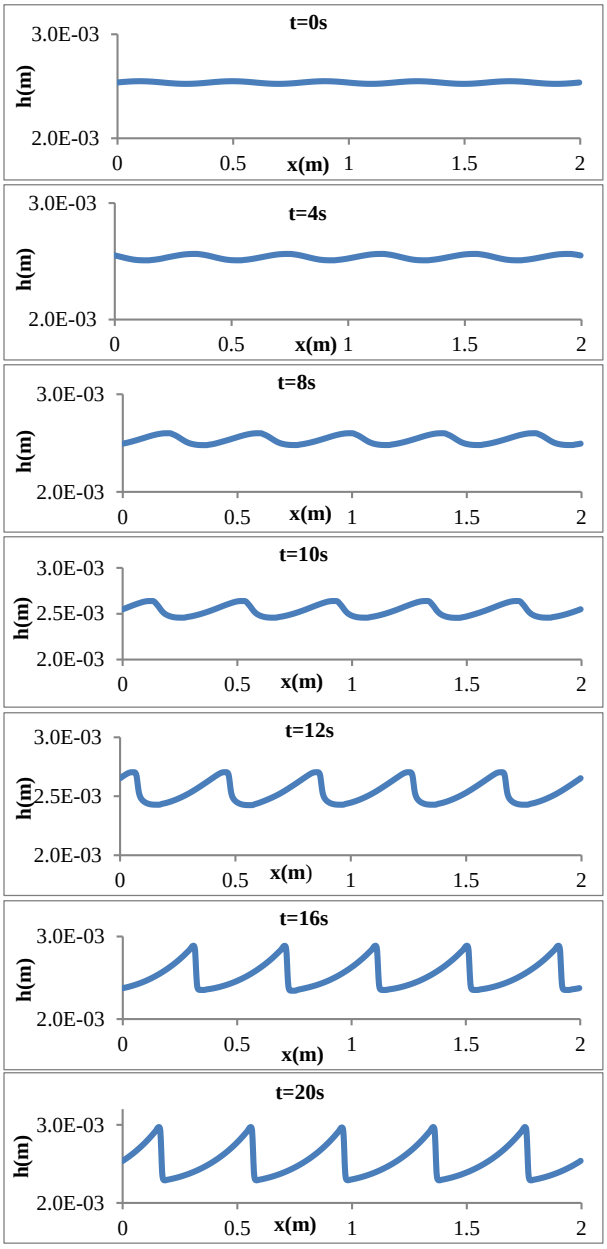

Figure 6. The results of the present model for evolution of roll-waves.

Figure 7 shows the comparison of the present model results and the analytical solution of Dressler [8]. It can be observed that good agreement is achieved. The value of Root Mean Square Error (RMSE) is equal to 1.2×10^{-5} m according to the present model results in this test.

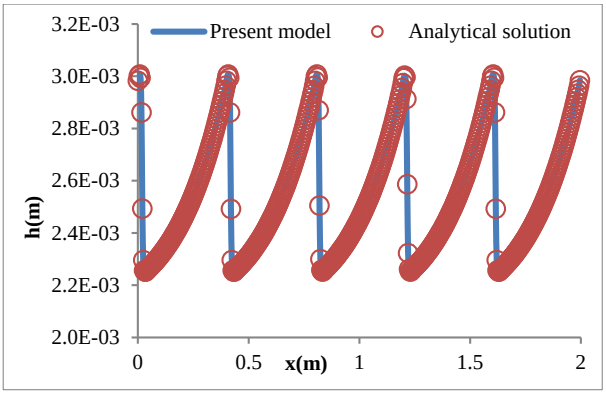

Figure 7. Comparison of the result of the present model and analytical solution of Dressler.

4. Conclusion

This research has focused on the treatment of the source term and modeling the tidal flow over wavy bed and the evolution of the roll-waves using the 1D shallow water equations. The TVD-WAF method with second-order accuracy both in space and time is applied for modeling fluxes at the interface of the cells. The Splitting scheme for equations with source terms is selected and the trapezoidal time integration method is employed. A set of three initial value sub-problems is used. Each numerical sub-problem is dealt with separately for a time step $\Delta t'$ (to achieve the second-order accuracy). First, the homogeneous advection problem is solved and then the ordinary differential equation is solved with the initial data taken from the solution of the previous step. Finally the ODE is solved and the depth and velocity are calculated at the new time level. This procedure for solving inhomogeneous system is simpler and efficiently significant. Model verification has been made by comparison of the model results with the exact solution of the dam-break problem. Then the tidal wave and roll-waves are modeled. Comparison of the results shows that the present model results are in good agreement with the corresponding analytical solutions.

5. References

[1] Toro, E. F., *Riemann solver and numerical methods for fluid dynamics*, Springer, Berlin, 1999.

[2] Kim, SD., Lee, HJ., Jeung, I. and Choi, J., "Realization of contact resolving approximate Riemann solvers for strong shock and expansion flows", *International Journal for Numerical Methods in Fluids*, 2010, 62, 10, pp. 1107-1133.

[3] Quirk, JJ., "A contribution to the great Riemann solver debate", *International Journal for Numerical Methods in Fluids*, 1994, 18, 6, p. 555-574.

[4] Zhou, J. G., Causon, D. M., Mingham, C. G. & Ingram, D. M., "The surface gradient method for the treatment of source terms in the shallow water equations", *Journal of Computational Physics*, 2001, 168, 1, pp. 1-25.

[5] Pu, J. H., Cheng, N., Tan, S. K., Shao, S., "Source term treatment of SWEs using surface gradient upwind method", *journal of Hydraulic Research*, 2012, 50, 2, pp. 145-153.

[6] Devkota, J., Fang, X., "Numerical simulation of flow dynamics in a tidal river under various upstream hydrologic conditions", *Hydrological Sciences Journal*, 2015, 60, 10, pp. 1666-1689.

[7] Huang, J., Zhang, X., Chua, V., "Numerical modeling of longitudinal dispersion in tidal flows with submerged vegetation", *journal of Hydraulic Research*, 2015, 53, 6, pp. 728-746.

[8] Dressler, R. F., "Mathematical solution of the problem of roll waves in inclined channel flows", *Commun. Pure Appl. Maths*, 1949, 2, pp. 149–194.

[9] Que, Y.T. & Xu, K., "The numerical study of roll-waves in inclined open channels and solitary wave run-up", *International Journal for Numerical Methods in Fluids*, 2006, 50, 9, pp. 1003-1027.

[10] Toro, E. F., Spruce, M., Speares, W.,"Restoration of the contact surface in the HLL Riemann solver", *Shock Waves*, 4, 1, 1994, pp. 25-34.

[11] Toro, E. F., *Shock Capturing Method For Free Surface Shallow Flows*, John Wiley and Sons, 2001.

[12] Toro, E. F., *Riemann solvers and numerical methods for fluid dynamics*, Springer, third Edition, 2009.

[13] Mahdavi, A. & Talebbeydokhti, N., "Modeling of Non-Breaking and Breaking Solitary Wave Run-Up Using Shock-Capturing TVD-WAF Scheme", *Journal of Civil Engineering*, 2011, 15, 6, pp. 945-955.

[14] Bermudez, A., Vazquez-Cendon, M. E., "Upwind methods for hyperbolic conservation laws with source term", *Comput. Fluids*, 23, 7, 1994, pp. 1049-1071.